Nanoscale

PAPER

View Article Online
View Journal | View Issue

Cite this: *Nanoscale*, 2021, **13**, 7334

Concentrated small extracellular vesicles from menstrual blood-derived stromal cells improve intrauterine adhesion, a pre-clinical study in a rat model†

Siwen Zhang,‡[a,b] Qiyuan Chang,‡[a,b] Pingping Li,[a,b] Xiaoyu Tong,[c,d] Yi Feng,[c,d] Xinyao Hao,[a,b] Xudong Zhang,[a,b] Zhengwei Yuan[e] and Jichun Tan *[a,b]

We previously reported that transplantation of menstrual blood-derived stromal cells (MenSCs) significantly improved fertility restoration in intrauterine adhesion (IUA). However, it is difficult to obtain menstrual blood samples in some severe IUA patients who have amenorrhea or oligomenorrhea. Thus, a safe and effective stem cell replacement therapy is necessary to promote endometrial regeneration. Recent studies demonstrated that the effects of MenSCs are partly mediated in a paracrine manner *via* small extracellular vesicles (sEVs). To explore this possibility, we performed a pre-clinical study to investigate whether concentrated MenSC-derived sEVs (MenSCs-sEVs) are sufficient to repair IUA and the mechanisms underlying their action. Rat IUA models were established by mechanical injury, followed by the administration of MenSCs or MenSCs-sEVs through intrauterine transplantation. Consistent with the efficacy of MenSCs, MenSCs-sEVs effectively recovered the morphology, promoted regeneration of the glands and angiogenesis, and reversed endometrial fibrosis in the IUA uterus. The endometrial receptivity and pregnancy outcome significantly improved after repeated MenSCs-sEVs transplantations. In addition, all rats in the MenSCs-sEVs group had no hematological or biochemical abnormalities. Three-dimensional fluorescence imaging suggested that MenSCs tended to migrate through the bloodstream, whereas MenSCs-sEVs had a better localized therapeutic effect. Moreover, MenSCs and MenSCs-sEVs inhibited the TGFβ1/SMAD3 pathway in the IUA endometrium, while promoting the phosphorylation of SMAD1/5/8 and ERK 1/2 and upregulating the expression of BMP7. Thus, MenSCs-sEVs safely and effectively enhanced endometrial restoration, suggesting a promising non-cellular therapy for endometrial regeneration and a key role in MenSC-mediated IUA treatment.

Received 18th December 2020,
Accepted 2nd March 2021

DOI: 10.1039/d0nr08942g

rsc.li/nanoscale

Introduction

Intrauterine adhesion (IUA), also called Asherman's syndrome, is a major cause of female secondary infertility. IUA is characterized by hypomenorrhea, amenorrhea, infertility, and recurrent miscarriages, and is often linked to endometrial damage caused by intrauterine operation.[1] In patients with severe IUA, it is difficult to restore fertility with conventional therapeutic methods such as hysteroscopic adhesiolysis and hormone supplementation.[2]

Recently, the therapeutic effects of mesenchymal stem cells (MSCs) transplantation have been demonstrated for IUA. MSCs derived from the bone marrow, umbilical cord, uterine endometrium, and oral mucosa have been investigated for their endometrial regeneration potential.[3–5] Menstrual blood-derived stromal cells (MenSCs) are endometrial MSCs derived from menstrual blood shedding. These cells are readily available, non-invasively collected, and ethically sound. These advantages indicate the potential for the widespread appli-

[a]*Center of Reproductive Medicine, Department of Obstetrics and Gynecology, Shengjing Hospital of China Medical University, Shenyang 110022, China. E-mail: tjczjh@163.com, zhangsiwenivy@foxmail.com, shelleychang1994@163.com, lipingping0227@163.com, 547087434hxy@gmail.com, cmuzxdlucky@163.com; Tel: +86 18940251868*
[b]*Key Laboratory of Reproductive Dysfunction Diseases and Fertility Remodeling of Liaoning Province, Shenyang 110022, China*
[c]*Department of Integrative Medicine and Neurobiology, School of Basic Medical Sciences, Institutes of Brain Science, Brain Science Collaborative Innovation Center, State Key Laboratory of Medical Neurobiology, Institute of Acupuncture and Moxibustion, Fudan Institutes of Integrative Medicine, Fudan University, Shanghai 200032, China. E-mail: 17211010071@fudan.edu.cn, fengyi17@fudan.edu.cn*
[d]*Shanghai Key Laboratory of Acupuncture Mechanism and Acupoint Function, Shanghai 200032, China*
[e]*Key Laboratory of Health Ministry for Congenital Malformation, Shengjing Hospital of China Medical University, Shenyang 117004, China. E-mail: yuanzw@hotmail.com*

†Electronic supplementary information (ESI) available. See DOI: 10.1039/d0nr08942g

‡These authors contributed equally to this study.

cation of MenSCs in regenerative medicine.[6] In our previous clinical study, seven patients with severe IUA achieved significant endometrial restoration and morphological uterine recovery after autologous MenSCs transplantation, and four of these patients eventually became pregnant.[7] Moreover, we demonstrated that MenSCs could markedly accelerate endometrial repair and promote fertility restoration in IUA model rats.[8]

Notably, only a few green fluorescent protein (GFP)-positive MenSCs were detected in the endometrium of the IUA rats, suggesting that in addition to their autonomous proliferation and differentiation into the tissue, MenSCs may also exert their therapeutic effects on tissues through other biological mechanisms. Recent studies further suggested that the underlying mechanism of MSC-based therapies may involve paracrine secretion, mainly through the release of numerous extracellular vesicles (EVs).[9] EVs are particles naturally released from the cell that are delimited by a lipid bilayer without a functional nucleus.[10] EVs contain large amounts of proteins and genetic materials (mRNAs, microRNAs, and other non-coding RNAs) that are transferred and released into the target cells, where they play key roles in cellular signaling. The lipid bilayer membrane protects their contents and enables them to travel long distances through tissues.[11,12] Indeed, EVs have been shown to participate in MSC-mediated tissue regeneration by delivering their contents to damaged cells or tissues. The therapeutic potential of MSC-derived EVs in cell-free regenerative medicine, including wound and liver repair, has been demonstrated in multiple studies.[13,14]

In this study, we evaluated whether MenSC-derived EVs (MenSCs-sEVs) are sufficient for MenSC-mediated IUA repair and endometrial regeneration. The therapeutic effects of MenSCs and MenSCs-sEVs were compared by pathological staining, protein expression, endometrial receptivity assessment, and fertility improvement in a rat model of IUA. The safety of MenSCs-sEVs transplantation was further evaluated based on blood test results. In addition, we used tissue clearing technology and three-dimensional (3D) imaging to investigate the mechanism by which MenSCs and MenSCs-sEVs restore the endometrium. Our study provided a theoretical basis for the use of MenSCs-sEVs as a cell-free treatment for patients with IUA.

Materials and methods

Ethical approval

All protocols were approved by the Ethics Committee of the Shengjing Hospital of China Medical University (2019PS349K) and were consistent with the principles of the Declaration of Helsinki.

Isolation and characterization of MenSCs and MenSCs-sEVs

In this study, the MenSCs were separated from menstrual blood samples of three healthy female volunteers (aged 25–30 years old). They voluntarily provided menstrual blood samples for this study and signed informed consent forms. Menstrual blood samples were collected after vaginal disinfection. The isolation and culture of MenSCs were executed in the same way as in our previous study;[8] P3–P6 MenSCs were used in this study. EVs were isolated from the supernatant of cultured MenSCs and characterized using different methods, including transmission electron microscopy (TEM), nanoparticle tracking analysis (NTA), western blotting, shotgun proteomics and gene ontology (GO) annotation. The enriched pathways were visualized using Cytoscape (v3.5.0) and ClueGO (v.2.5.0), associated with the Kyoto Encyclopedia of Genes and Genomes (KEGG) database.[15] Detailed methods of isolation, characterization, shotgun proteomic and bioinformatics analyses of MenSCs-sEVs are given in ESI 1.† P3–P6 MenSCs were labeled with GFP by lentiviral transfection (MOI 20) before transplantation.

Rat IUA model establishment and treatment

Female Sprague-Dawley rats (200–220 g, 10-week-old) were purchased from HFK Bioscience Co. (Beijing, China). The rats were housed in an environment with a 12/12 h light/dark cycle, a temperature of 22 ± 1 °C, and a relative humidity of 50 ± 1%. The establishment and treatment of a rat IUA model were carried out using a previously described method.[8] Briefly, 54 rats with regular estrous cycles were anesthetized by 3% sodium pentobarbital (1 ml kg^{-1}), and then an incision which could pass through a 16-gauge syringe was performed on the uterus using ophthalmic scissors. The uterine endometrium of both laterals was scratched by the syringe until the uterine walls became rough and pale. The uterine cavity was washed with sterile normal saline before closing. After two estrous cycles (about 9 days), all rats that received intrauterine mechanical injury were randomly divided into three groups: Sham group, MenSCs group, and MenSCs-sEVs group. After the mice are anesthetized and the uterus is exposed, we use 30-gauge syringes to inject 50 μl of the treatment liquid under the uterine serous membrane at multiple points, carefully avoiding the leakage of the liquid from the uterus. The MenSCs group received 5×10^5 MenSCs suspended in 50 μl PBS per uterus. The MenSCs-sEVs group received 2.125×10^7 particles of MenSCs-sEVs released from 5×10^5 MenSCs suspended in 50 μl PBS (4.25×10^8 particles per mL, 300 μg mL^{-1}) per uterus. The Sham group received the same volume of PBS (placebo) per uterus. Six rats without operation constituted the normal group. Rats were sacrificed 4.5, 9 or 18 days after treatment.

Hematology test and serum biochemical test

In the same method as in our previous study,[16] freshly collected rat peripheral venous blood after 4.5 days of treatment in both MenSCs and MenSCs-sEVs was tested for hematology composition (Procyte DX, IDEXX Laboratories, USA, $n = 5$). Red blood cells, hematocrit, hemoglobin, average red blood cell volume, average hemoglobin concentration, red blood cell distribution width, reticulocytes, white blood cells, neutrophils, lymphocytes, monocytes, eosinophils, basophils, and platelet related concentrations or percentages were evaluated. Freshly separated serum was tested for urea, creatinine, total protein,

albumin, globulin, alanine aminotransferase, aspartate aminotransferase, alkaline phosphatase, and sodium, potassium, and chloride ion concentrations (Catalyst One, IDEXX Laboratories, USA, n = 5). 5 healthy SD rats were assigned as the normal group.

Fertility test

In contrast to the previous treatment usage, rats in the MenSCs-sEVs group used in the pregnancy test were given MenSCs-sEVs graft per estrous cycle for a total of four times. Twenty-eight days after the first treatment, different groups of IUA rats (n = 4) were mated with healthy male rats (2 : 1) at 21:00 p.m. each day, and vaginal smears were performed at 09:00 a.m. the following day. If the sperm was positive, the female rats were considered to have successfully mated at E0.5 and were then housed separately. The pregnant female rats were sacrificed on E13.5; the number and size of the embryos were recorded.

Histological analysis

Uterus tissues from each group were fixed in 4% neutral buffered formalin, dehydrated, and then embedded in paraffin. Serial sections of 5 μm were sliced and then stained with hematoxylin and eosin (H&E) for morphological assessment under a light microscope (n = 6). Each slice was randomly selected to measure endometrial thickness in 4 fields using ImageJ software (National Institutes of Health, USA). Annular structures containing intact cuboidal epithelium were considered as glands. The total number of glands was counted under a magnification of ×100. Masson trichrome staining (Solarbio, China, Cat#G1340) was utilized to assess fibrosis and normal uterine sections were used as a negative control. The percentage of blue staining area of fibrosis was measured using ImageJ software.

Immunohistochemistry

To evaluate the cell proliferation of endometrium after treatment of 4.5 days, the Ki-67 expression was identified by immunohistochemistry (n = 6). Sections of the uterus were deparaffinized and gradually dehydrated. Antigen retrieval was performed in sodium citrate buffer using microwave heating. After endogenous peroxidase was inhibited for 15 min and protein blocking for 30 min at 37 °C, anti-Ki67 (1 : 100; Abcam, UK, Cat#ab16667) was added and incubated at 4 °C overnight. Then the sections were incubated with a secondary antibody for 2 h at room temperature. The sections were exposed to DAB to visualize the bound antibody before counterstaining with Mayer's hematoxylin. The slides were viewed and photographed under a microscope and the total nuclear staining number of Ki67 was counted using Image-pro Plus (Media Cybernetics, MD, USA).

Western blotting

Total protein of uterine tissue was extracted using RIPA lysis buffer (Beyotime, China, Cat#P0013B), and the protein concentration was quantified by BCA assay. Equal amounts of protein samples of 4.5 days were separated on SDS-PAGE gel (Beyotime, China, Cat#P0012A), and then transferred onto PVDF membranes (Millipore, Billerica, MA, USA). After blocking with 5% skimmed milk, the membranes were incubated with primary antibodies against collagen I (1 : 1000, Abcam, UK, Cat#ab34710), VEGFA (1 : 1000, Wanleibio, China, Cat#WL00009b), LIF (1 : 1000, Absin, China, Cat#abs110821), ITGAV (1 : 1000, Absin, China, Cat#abs136335), bone morphogenetic protein 7 (BMP7, 1 : 500, Proteintech, China, Cat#12221-1-AP), transforming growth factor β1 (TGFβ1, 1 : 500, Proteintech, China, Cat#21898-1-AP), SMAD3 (1 : 500, Proteintech, China, Cat#25494-1-AP), phospho-SMAD3 (1 : 500, CST, USA, #9520), SMAD1/5/8 (1 : 500, Immunoway, China, Cat#YT6085), phospho-SMAD1/5/8 (1 : 1000, CST, USA, #13820), extracellular-regulated kinase 1/2 (ERK1/2, CST, USA, #4695), phospho-ERK1/2 (CST, USA, #4370) and GAPDH (1 : 2000, Goodhere, China, Cat#AB-P-R-00) overnight at 4 °C. Then the membranes were incubated with HRP-conjugated secondary antibodies (Beyotime, China, Cat#A0208) and scanned with a Darkroom Eliminator (Azure Biosystems, USA, Cat#C300) using ECL (Beyotime, China, Cat#P0018).

Tissue clearing, immunofluorescence staining and image acquisition

After 4.5 days of MenSCs or MenSCs-sEVs treatment, bioluminescence imaging (BLI, MS FX Pro system, Carestream, USA) was used to detect the fluorescence signals in the main organs (brain, heart, lungs, liver, spleen, kidneys, uterus and ovaries) of the IUA rat. For tissue clearing, we used the CUBIC clearing method described by Ma *et al.*[17] Rat uterus was carefully dissected and immersed in 4% PFA for 24 h at 4 °C. Then the tissues were washed with shaking with PBS/0.01% sodium azide for 4 h at 37 °C to remove PFA. The tissues were cleared with diluted reagent 1 with shaking for 3 h at 37 °C until a satisfying optical transparency was achieved. Then the samples were washed with PBS/0.01% sodium azide for 2 h and three times. For immunofluorescence staining, the samples were incubated with primary antibodies (1 : 20, PECAM1 and CK-18) for 48 h, washed in PBS for 24 h, and then incubated with secondary antibodies for 48 h, all with shaking at 37 °C. Next, the samples were cleared with diluted reagent 2 with shaking at 37 °C and transferred to reagent 2 for at least 1 day until they turned totally clear. The cleared samples were stored in reagent 2 at 4 °C until imaging. All performance were in dark condition. For image acquisition, we used an 18 light sheet illumination microscope (LS18, Nuohai Life Science) to collect the raw images of the samples. The data were saved in CZI format after scanning. Arivis software (Arivis AG, München, Germany) was used to transform the data into TIFF format. Imaris software (v.8.0, Bitplane, Zurich, Switzerland) was used to analyse and rebuild the digital images.

Statistical analysis

All data were presented as mean ± standard deviation (SD), and one-way analysis of variance (ANOVA) was utilized to

analyze the comparisons among rat groups. The recognized statistically significant differences were assessed by Bonferroni *post hoc* tests, and the analyses were performed using Prism 8 software (GraphPad, San Diego, USA). $P < 0.05$ was considered to represent a statistically significant difference.

Results

Characterization and proteomic analysis of MenSCs-sEVs

EVs were isolated from the supernatant of cultured MenSCs and characterized using different methods, including transmission electron microscopy (TEM), nanoparticle tracking analysis (NTA), and western blotting. NTA and TEM revealed that the EVs had a concentration of 1.7×10^9 particles per mL and a peak diameter of 127 nm (Fig. 1A), and exhibited a typical cup- or sphere-shaped morphology (Fig. 1B). Western blotting confirmed that the protein markers of EVs, CD63 and CD81 were expressed in EVs derived from the culture supernatant of MenSCs (Fig. 1C). These data were consistent with the description of small extracellular vesicles (sEVs) in MISEV2018.[10] Therefore, in this study, we named the EVs obtained from the MenSCs culture supernatant as MenSCs-sEVs.

Shotgun proteomics and Gene Ontology (GO) annotation were performed on the obtained MenSCs-sEVs. A total of 1131 exosomal proteins were analyzed, which were predicted to be involved in cellular components, biological processes, and molecular functions. The top five GO categories for biological processes were cellular process, biological regulation, metabolic process, regulation of biological process, and response to stimulus (Fig. 1D). To further explore the enriched pathways associated with MenSCs-sEVs proteins, all proteins were imported into the ClueGO app on the Cytoscape platform to create a network of the over-represented GO terms. Only significant terms (p-value < 0.05) were displayed, and were annotated using the Kyoto Encyclopedia of Genes and Genomes (KEGG) database as a reference. Multiple functions of these proteins were identified, including those related to regulation of growth (71), the Wnt signaling pathway (52), angiogenesis (40), epithelium development (97), wound healing (76), collagen fibril organization (18), extracellular matrix (ECM)–receptor interaction (32), PI3K-Akt signaling pathway (43), and integrin-mediated signaling pathway (37) (Fig. 1E).

MenSCs-sEVs exhibited more local retention in the uterus compared to MenSCs

To enable tracing of the grafts, the MenSCs were transfected with green fluorescent protein (GFP) and the MenSCs-sEVs were labeled with CM-DiI. The fluorescence signal distributions of the grafts in the uterus and other organs were then observed by bioluminescence imaging. The GFP fluorescence was distributed throughout the IUA uterus at 4.5 days after MenSCs injection, and a high-intensity signal was detected in the uterus near the vagina. In contrast, after MenSCs-sEVs transplantation, DiI fluorescence was observed at multiple points in the IUA uterus, and the high-density signal was confined to the region around the injection area (Fig. 2A). After MenSCs transplantation, higher GFP signals were detected in the brain and liver than in the uterus, whereas the DiI signal of MenSCs-sEVs was much higher in the uterus than in other organs of the rats (Fig. 2B).

Intrauterine transplantation of MenSCs-sEVs would not cause hematological or biochemical abnormalities

To determine the safety of MenSCs-sEVs transplantation, we collected peripheral blood from the IUA rats at day 4.5 post-treatment for the examination of the blood cell composition and serum biochemistry. Intrauterine transplantation of aseptically prepared MenSCs-sEVs did not cause any abnormalities to the hematocrit of the IUA rats (Table 1). Likewise, the liver and kidney metabolic parameters, as well as serum Na, K, and Ca ion concentrations in the MenSCs-sEVs group were within the normal reference range (Table 2). These results indicated that intrauterine transplantation of MenSCs-sEVs was safe.

MenSCs-sEVs transplantation recovered the morphology and promoted the proliferation of endometrial cells in the IUA uterus

To examine whether MenSCs-sEVs have therapeutic effects for IUA, we used the mechanically injured rodent model established in our previous study.[8] The morphology of the rat uterus was observed using hematoxylin and eosin staining (Fig. 3A–C). The endometrial thickness was measured, and the glands were counted at day 4.5, 9, and 18 after a single phosphate-buffered saline (PBS), MenSCs, or MenSCs-sEVs transplantation (Fig. 3D and E). As compared to the Sham group, significant increases in endometrial thickness were observed after either MenSCs or MenSCs-sEVs transplantation on days 4.5, 9, and 18 (all $p < 0.0001$). Endometrial thickness steadily and significantly increased throughout the evaluation period in the MenSCs group. However, compared with that measured on day 4.5, there were no further increases in endometrial thickness observed on days 9 and 18 in the MenSCs-sEVs group. By day 18, the endometrial thickness in the MenSCs group was significantly higher than that in the MenSCs-sEVs group ($p = 0.0180$). Similarly, as compared to the Sham group, significantly increased gland numbers were detected in the MenSCs and MenSCs-sEVs groups on days 4.5, 9, and 18 (both $p < 0.001$). On day 18, the number of glands in the MenSCs group was significantly higher than that in the MenSCs-sEVs group ($p = 0.0030$).

Cell proliferation in the endometrium was evaluated using immunohistochemistry. At 4.5 days after MenSCs and MenSCs-sEVs transplantation, the expression of the proliferation marker Ki-67 was detected in the IUA endometrium, which was mainly concentrated in the epithelial cells (Fig. 3F), particularly the luminal epithelial cells. Compared with the Sham group, the number of Ki-67-positive cells was significantly increased in the MenSCs and MenSCs-sEVs groups (both $p < 0.0001$; Fig. 3G). The number of Ki-67-positive cells was also higher in the MenSCs-sEVs group than that in the MenSCs group ($p = 0.0035$). These results demonstrated that

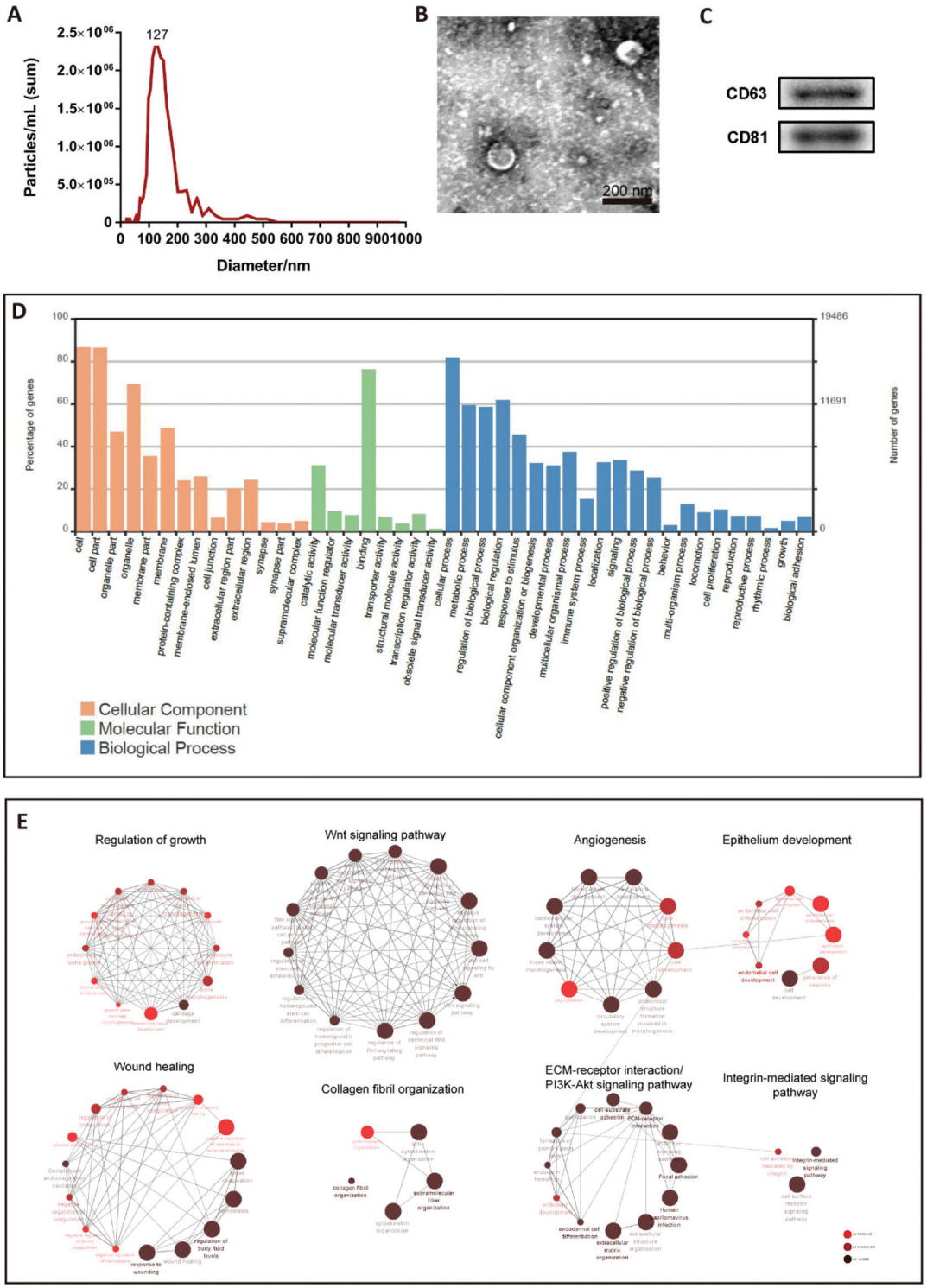

Fig. 1 Characterization, gene ontology (GO) enrichment and Cytoscape based ClueGo/CluePedia pathway analysis of MenSCs-sEVs. (A) Size distribution examined by nanoparticle tracking analysis (NTA); (B) morphology observed by transmission electron microscopy (TEM), scale bar = 200 nm; (C) western blot of the EV surface markers CD63 and CD81; and (D) GO analysis of MenSCs-sEVs proteins was classified by the biological processes, molecular functions and cellular components. (E) Pathway analysis and visualization of MenSCs-sEVs based on ClueGo/CluePedia. Enriched pathways were obtained from the Kyoto Encyclopedia of Genes and Genomes (KEGG) database. Terms for every node are grouped based on shared genes (kappa score). The degree of red represents the significance of the terms.

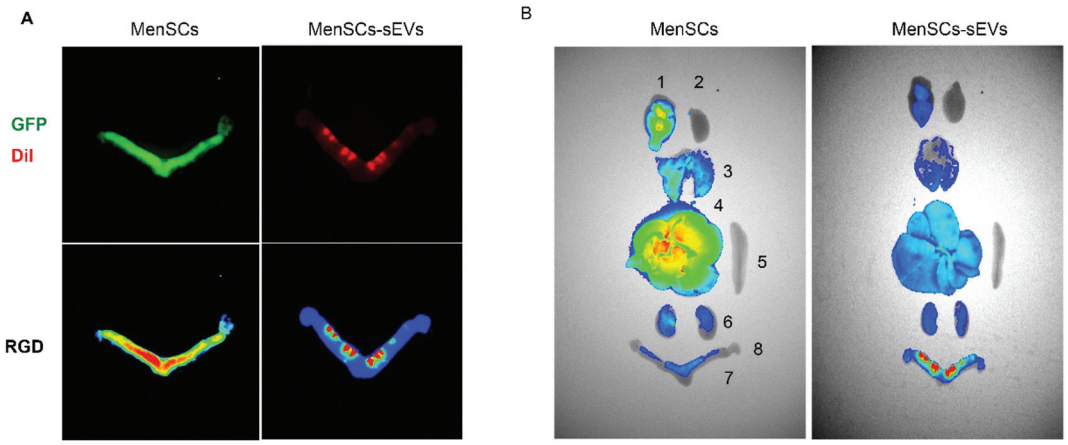

Fig. 2 Fluorescence localization of MenSCs and MenSCs-sEVs in the organs of IUA rats. (A) Location of MenSCs (GFP-green) and MenSCs-sEVs (DiI-red) in the uterus and (B) location of MenSCs and MenSCs-sEVs in the main organs (1: brain; 2: heart; 3: lungs; 4: liver; 5: spleen; 6: kidneys; 7: uterus; and 8: ovary).

Table 1 Hematological values of rats

Parameters	Normal	MenSCs	MenSCs-sEVs
RBC ($\times 10^{12}$ L^{-1})	7.20 ± 0.09	7.30 ± 0.19	7.26 ± 0.25
HCT (%)	39.32 ± 0.74	37.76 ± 0.87	40.74 ± 0.56
MCV (fL)	54.64 ± 0.54	52.76 ± 0.88	55.06 ± 2.60
MCH (pg)	18.66 ± 0.11	18.28 ± 0.54	18.18 ± 0.51
MCHC (g dL^{-1})	34.18 ± 0.53	34.60 ± 0.52	34.12 ± 0.23
RDW (%)	16.18 ± 0.33	17.30 ± 0.60	17.78 ± 0.69
RETIC (K μL^{-1})	3.86 ± 0.09	3.64 ± 0.61	3.76 ± 0.96
RETIC	277.00 ± 8.45	255 ± 31.51	283.70 ± 70.93
WBC ($\times 10^{12}$ L^{-1})	7.64 ± 1.67	7.83 ± 1.36	9.44 ± 0.63
NEU (%)	13.72 ± 4.22	13.38 ± 3.53	14.14 ± 3.38
LYM (%)	78.32 ± 5.45	75.48 ± 5.90	77.79 ± 6.52
MONO (%)	5.18 ± 0.83	7.44 ± 0.64	6.54 ± 1.07
EOS (%)	0.60 ± 0.12	0.90 ± 0.35	0.58 ± 0.11
BASO (%)	0.14 ± 0.11	0.32 ± 0.15	0.22 ± 0.16
NEU ($\times 10^{9}$ L^{-1})	1.02 ± 0.29	1.37 ± 0.79	1.41 ± 0.41
LYM ($\times 10^{9}$ L^{-1})	6.18 ± 1.59	5.38 ± 2.78	7.72 ± 0.55
MONO ($\times 10^{9}$ L^{-1})	0.38 ± 0.04	0.47 ± 0.20	0.64 ± 0.12
EOS ($\times 10^{9}$ L^{-1})	0.05 ± 0.01	0.06 ± 0.01	0.06 ± 0.02
BASO ($\times 10^{9}$ L^{-1})	0.01 ± 0.01	0.02 ± 0.01	0.01 ± 0.01
PLT (K μL^{-1})	1209 ± 26.66	1141 ± 206.00	1132 ± 127.10
MPV (fL)	8.50 ± 0.10	8.44 ± 0.27	8.40 ± 0.10
PDW (fL)	8.50 ± 0.16	8.58 ± 0.08	8.40 ± 0.33
PCT (%)	0.91 ± 0.03	0.96 ± 0.14	0.95 ± 0.10

Values are expressed as mean ± SD, n = 5 per group.

both MenSCs and MenSCs-sEVs significantly promoted endometrial regeneration and increased gland numbers. MenSCs exhibited a continuous repair effect in the damaged endometrium, whereas the MenSCs-sEVs released from an equal amount of cells exhibited similar treatment efficacy within a shorter treatment time.

MenSCs-sEVs promote endometrial gland formation and angiogenesis in IUA rats

To gain a more comprehensive understanding of the roles of MenSCs and MenSCs-sEVs *in vivo*, we investigated the 3D distribution of GFP-labeled MenSCs and CM-DiI-labeled MenSCs-sEVs in the IUA uterus by dissecting uterine fragments and performing tissue clearing. In addition, we traced the uterine glands and blood vessels using CK18 and cluster of differentiation platelet and endothelial cell adhesion molecule 1 (PECAM1) as respective markers. In the Sham group, the uterine cavity was narrow and adherent, with only a thin endometrium observed containing few glands and blood vessels. However, after either MenSCs or MenSCs-sEVs treatment, the uterine cavity volume was expanded, the endometrium thickened, and the number of endometrial glands increased (Fig. 4A). In the MenSCs-sEVs group, labeled MenSCs-sEVs aggregated at the injection site. A portion of the MenSCs-sEVs specifically migrated to the regenerated glandular epithelium, and newly formed glands were clustered around the injection site (Fig. 4B). In addition, the distribution of blood vessels in the endometrium and myometrium increased after MenSCs and MenSCs-sEVs treatments, accompanied by an increased expression level of PECAM1. PECAM1 was mainly expressed in clusters in the MenSCs-sEVs group (Fig. 4C). Additionally, co-localization of GFP and PECAM1 was detected in the MenSCs group, with part of the GFP signal distributed along the blood vessels that were PECAM1-positive. No obvious GFP-labeled MenSCs aggregation was observed (Fig. 4D).

MenSCs-sEVs restore endometrial receptivity and improve the fertility of IUA rats

At 4.5 days after treatment, we examined the levels of endometrial receptivity markers by western blot analysis (Fig. 5A). MenSCs and MenSCs-sEVs transplantation resulted in significant increases in the protein levels of leukemia inhibitory factor (LIF; p = 0.0445 and p = 0.0189, respectively) and integrin subunit alpha V (ITGAV; p = 0.0251 and p = 0.0003, respectively) as compared to those of the Sham group. The expression level of ITGAV was significantly higher in the MenSCs-sEVs group than that in the MenSCs group (p = 0.0087). Notably, the expression level of vascular endothelial growth factor A

Table 2 Serum biochemical values of rats

Parameters	Normal	MenSCs	MenSCs-sEVs	Standard reference
UREA	6.22 ± 0.51	6.52 ± 0.48	6.00 ± 0.76	3.20–7.50 mmol L^{-1}
CREA	27.60 ± 5.13	35.60 ± 4.29	29.00 ± 6.89	4–57 mmol L^{-1}
BUN/CREA	55.80 ± 11.71	46.20 ± 4.49	51.60 ± 8.99	—
TP	60.80 ± 4.09	64.00 ± 6.75	60.40 ± 4.34	53–69 g L^{-1}
ALB	31.80 ± 2.68	33.20 ± 5.02	31.60 ± 3.21	30–48 g L^{-1}
GLOB	29.40 ± 1.82	31.00 ± 2.00	28.60 ± 2.07	15–28 g L^{-1}
ALT	35.00 ± 6.04	38.20 ± 3.83	31.20 ± 4.87	20–61 U L^{-1}
AST	73.40 ± 11.84	61.40 ± 11.37	71.80 ± 15.64	39–111 U L^{-1}
ALKP	143.80 ± 14.45	135.00 ± 30.31	99.80 ± 16.24	16–302 U L^{-1}
Na	143.20 ± 1.48	141.20 ± 2.95	141.60 ± 1.14	137–154 mmol L^{-1}
K	5.38 ± 0.58	5.62 ± 0.19	4.84 ± 0.23	4.10–6.50 mmol L^{-1}
CL	103.80 ± 2.39	106.80 ± 2.78	105.60 ± 3.98	96–107 mmol L^{-1}

Values are expressed as mean ± SD, n = 5 per group.

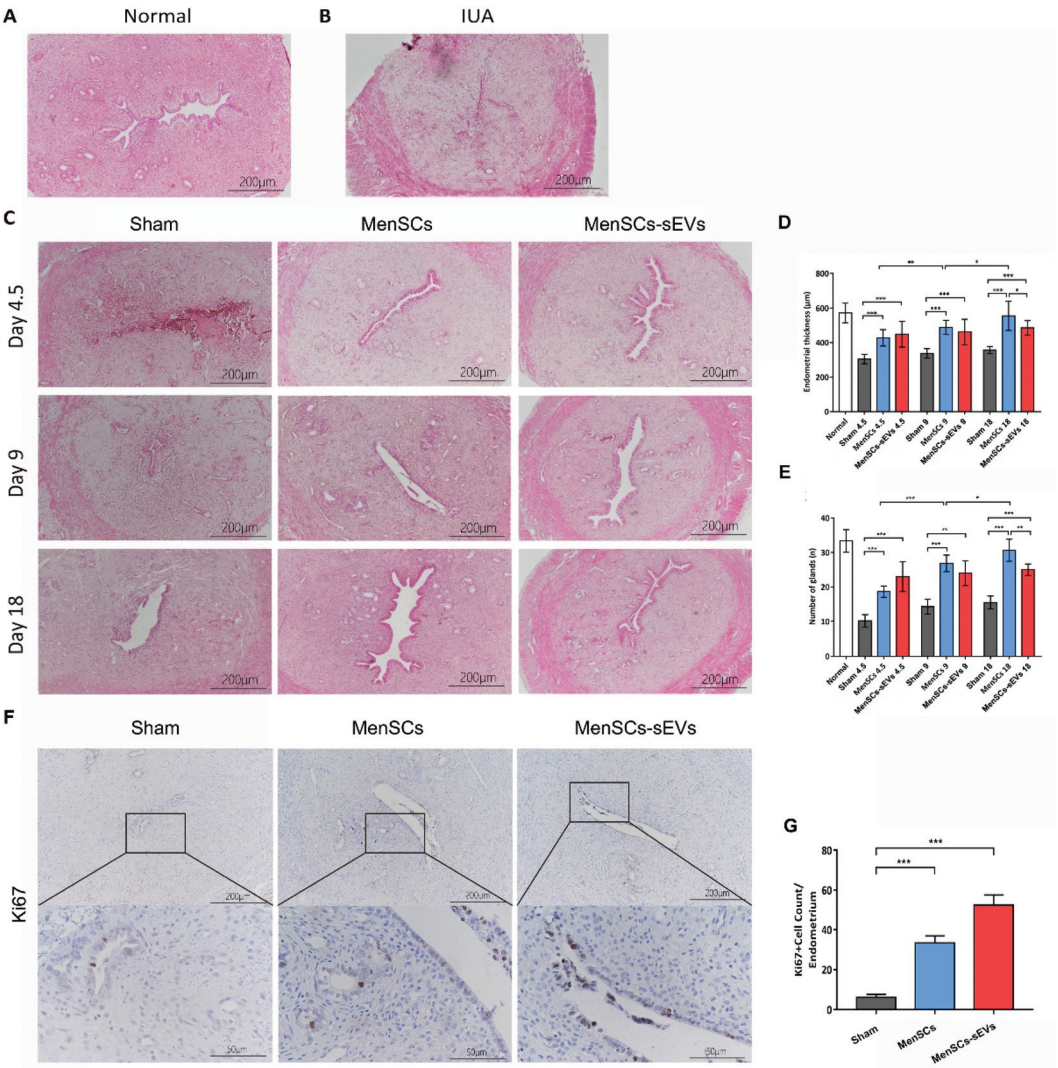

Fig. 3 MenSCs-sEVs promoted the morphological recovery of the endometrium. H&E staining of the uteri from the normal rat model (A) and the IUA rat model (B); (C) representative H&E staining of the uterus from the three groups after treatment for 4.5, 9 and 18 days, scale bars = 200 μm; (D) comparison of endometrial thickness (n = 6); (E) comparison of the number of glands (n = 6); (F) representative immunohistochemical staining of Ki-67 in the rat endometrium after treatment for 4.5 days, scale bars = 200 μm (upper images) and 50 μm (lower images); and (G) comparison of the nuclear staining number of Ki-67 ($n \geq 6$).

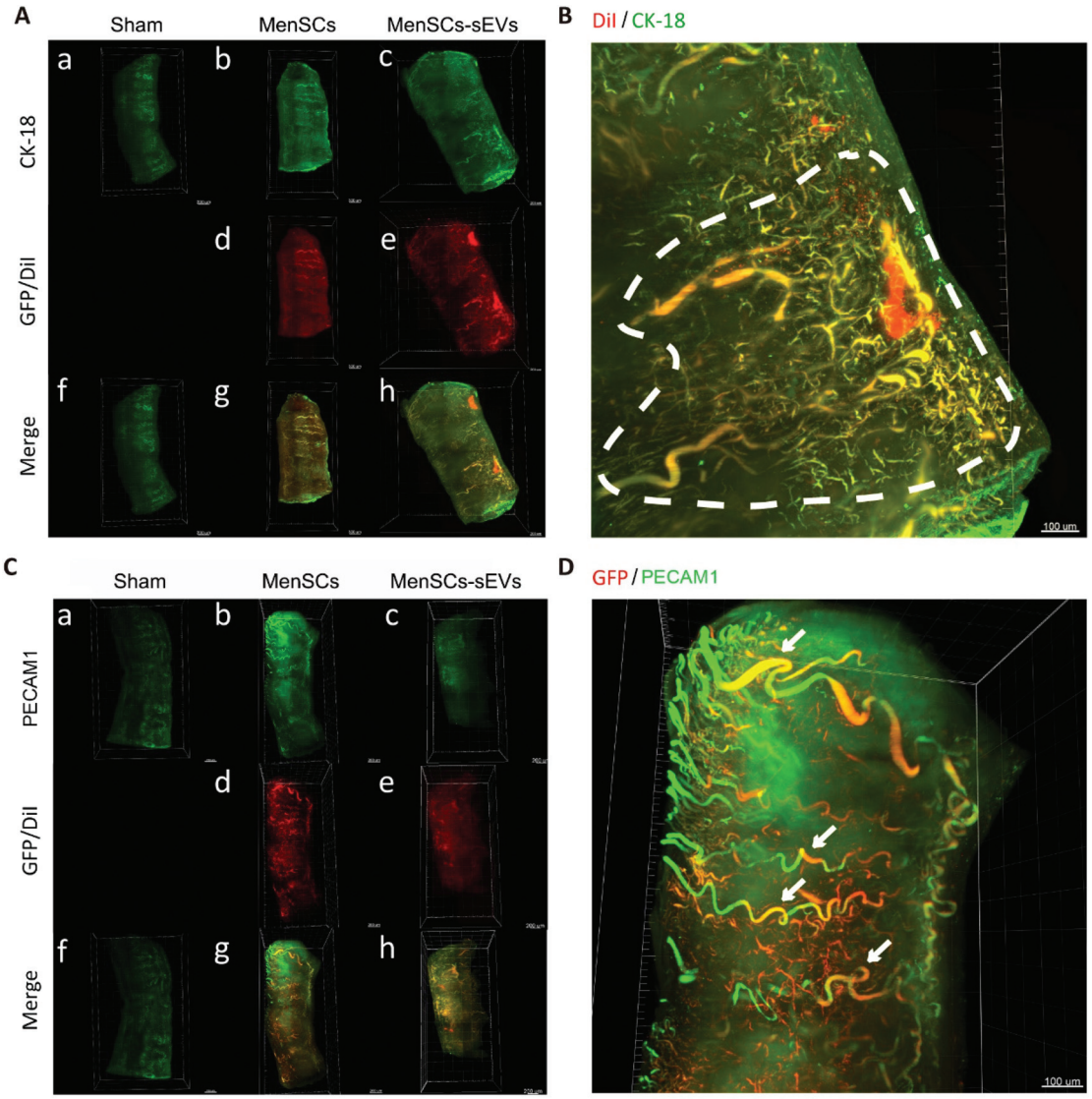

Fig. 4 MenSCs-sEVs promoted endometrial gland formation and angiogenesis in IUA rats by 3D imaging (A) 3D immunofluorescence image of the rat uterus labeled with CK-18, scale bars = 200 μm (a–c: CK-18, d: DiI, e: GFP, and f–h: merge). (B) Enlarged image of a–h. The dotted circles represent the clusters of regenerative glands, scale bars = 100 μm. (C) 3D immunofluorescence image of the rat uterus labeled with PECAM1, scale bars = 200 μm (a–c: PECAM1, d: DiI, e: GFP, and f–h: merge). (D) Enlarged image of c–g. The white arrow points to the co-localization of MenSCs and PECAM1, scale bars = 100 μm.

(VEGFA) was also significantly higher in the MenSCs-sEVs group ($p = 0.0396$; Fig. 5B).

To assess fertility after MenSCs and MenSCs-sEVs treatments, the number of embryos and their sizes were examined at E13.5. Compared with the Sham group (2.75 ± 0.85), there were significantly more embryos after either a single MenSCs intrauterine injection (11.75 ± 1.18, $p = 0.0008$) or four MenSCs-sEVs intrauterine transplantations (12.50± 1.32, $p = 0.0008$) (Fig. 5C and E). There were no differences in the live embryo size among the groups (Fig. 5D and F). These results indicated that both MenSCs and MenSCs-sEVs treatments could restore endometrial receptivity. In addition, repeated transplantation of MenSCs-sEVs could markedly improve fertility in IUA rats.

MenSCs-sEVs inhibit TGFβ1/SMAD3-mediated endometrial fibrosis by upregulating BMP7 expression and SMAD1/5/8 and ERK1/2 phosphorylation

Masson's trichrome staining was performed to assess fibrosis in the IUA-affected endometrium (Fig. 6A). Fibrosis was significantly reduced 4.5 days after the treatment in both the MenSCs ($p = 0.0002$) and MenSCs-sEVs ($p = 0.0001$) groups compared with that of the Sham group (Fig. 6B); there was no significant difference in fibrosis between the MenSCs-sEVs and MenSCs groups ($p = 0.1421$). Western blotting (Fig. 6C) showed that the collagen I expression level was significantly decreased in the MenSCs and MenSCs-sEVs groups as compared to the Sham group (both $p < 0.0001$; Fig. 6D). No signifi-

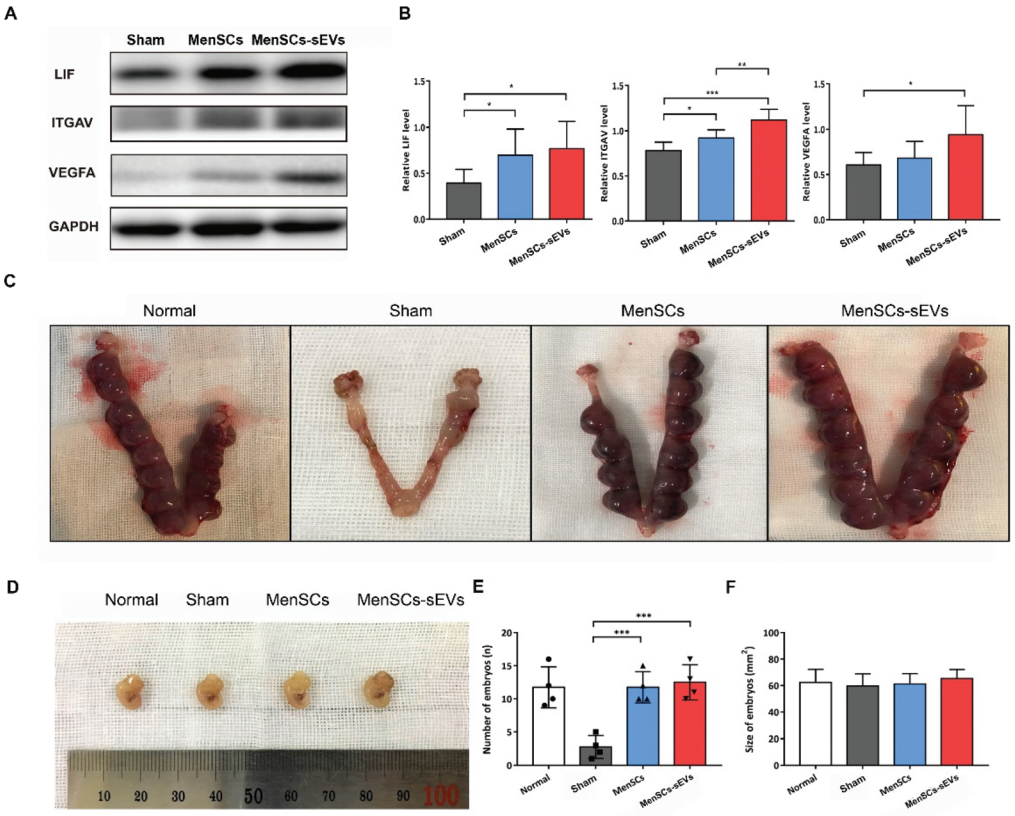

Fig. 5 MenSCs-sEVs improved endometrial receptivity and fertility of IUA rats. (A) Western blot analysis of the protein expression of LIF, ITGAV and VEGFA in the groups after treatment for 4.5 days; (B) statistical analysis of western blot ($n \geq 6$); (C) the rat uterus with embryo implantation at E13.5; (D) the embryo of the groups; (E) comparison of the number of embryos ($n = 4$); and (F) comparison of the size of the embryos ($n = 4$).

cant difference was observed between the MenSCs and MenSCs-sEVs groups ($p = 0.0812$). We next assessed the expression of proteins in the uterus by western blotting. MenSCs and MenSCs-sEVs transplantation resulted in decreases in TGFβ1 ($p = 0.0434$ and $p = 0.0334$, respectively) and phospho-SMAD3 ($p = 0.0398$ and $p = 0.0432$, respectively). The expression of ERK1/2 ($p_{ERK1} = 0.0117$, $p_{ERK2} = 0.0036$, and $p_{ERK1} = 0.0117$, $p_{ERK2} = 0.0183$, respectively), and phospho-ERK1/2 ($p_{pERK1} = 0.0286$, $p_{pERK2} = 0.0379$, and $p_{ERK1} = 0.0286$, respectively) were increased in the IUA uterus (Fig. 6E and F). After MenSCs and MenSCs-sEVs transplantation, there were significant increases in BMP7 ($p = 0.0348$ and $p = 0.0075$, respectively) and phospho-SMAD1/5/8 ($p = 0.026$ and $p = 0.0396$, respectively) in the IUA uterus (Fig. 5G and H). These results suggested that both MenSCs and MenSCs-sEVs reduced endometrial fibrosis by regulating BMP7, TGFβ1/SMAD signaling, and ERK signaling.

Discussion

In this study, we demonstrated that intrauterine transplantation of MenSCs-sEVs effectively restored the impaired endometrium by increasing its thickness, gland numbers, and vasculature in the IUA rat model. MenSCs-sEVs displayed injury tropism, as they migrated to the endometrial lesions to promote angiogenesis and gland regeneration. Moreover, repeated transplantation of MenSCs-sEVs significantly enhanced endometrial receptivity and improved the fertility of IUA rats. No death and hematological or biochemical abnormalities were observed after intrauterine transplantation of MenSCs-sEVs. Both the MenSCs and MenSCs-sEVs treatments significantly upregulated BMP7 expression and inhibited endometrial fibrosis mediated by the TGFβ1/SMAD3 pathway. In addition, increased phosphorylation of SMAD1/5/8 and ERK1/2 was detected after MenSCs and MenSCs-sEVs treatments. To the best of our knowledge, this is the first evidence demonstrating the therapeutic effects and safety of *in vivo* applications of MenSCs-sEVs in a rat model of IUA. In addition, this is the first attempt to detect the 3D distribution of labeled sEVs in the IUA rat uterus.

MSCs from different tissues, such as menstrual blood (MenSCs), the bone marrow (BMSCs), and the umbilical cord (UC-MSCs), have been extensively studied for their potential in tissue regeneration.[3–5] Transplantation of UC-MSCs and BMSCs has demonstrated excellent therapeutic outcomes in IUA models and clinical studies.[18,19] However, UC-MSCs are allogeneic and have ethical limitations, and the invasive retrieval process of BMSCs is associated with an increased risk of pain and infection. In contrast, MenSCs may be more suitable

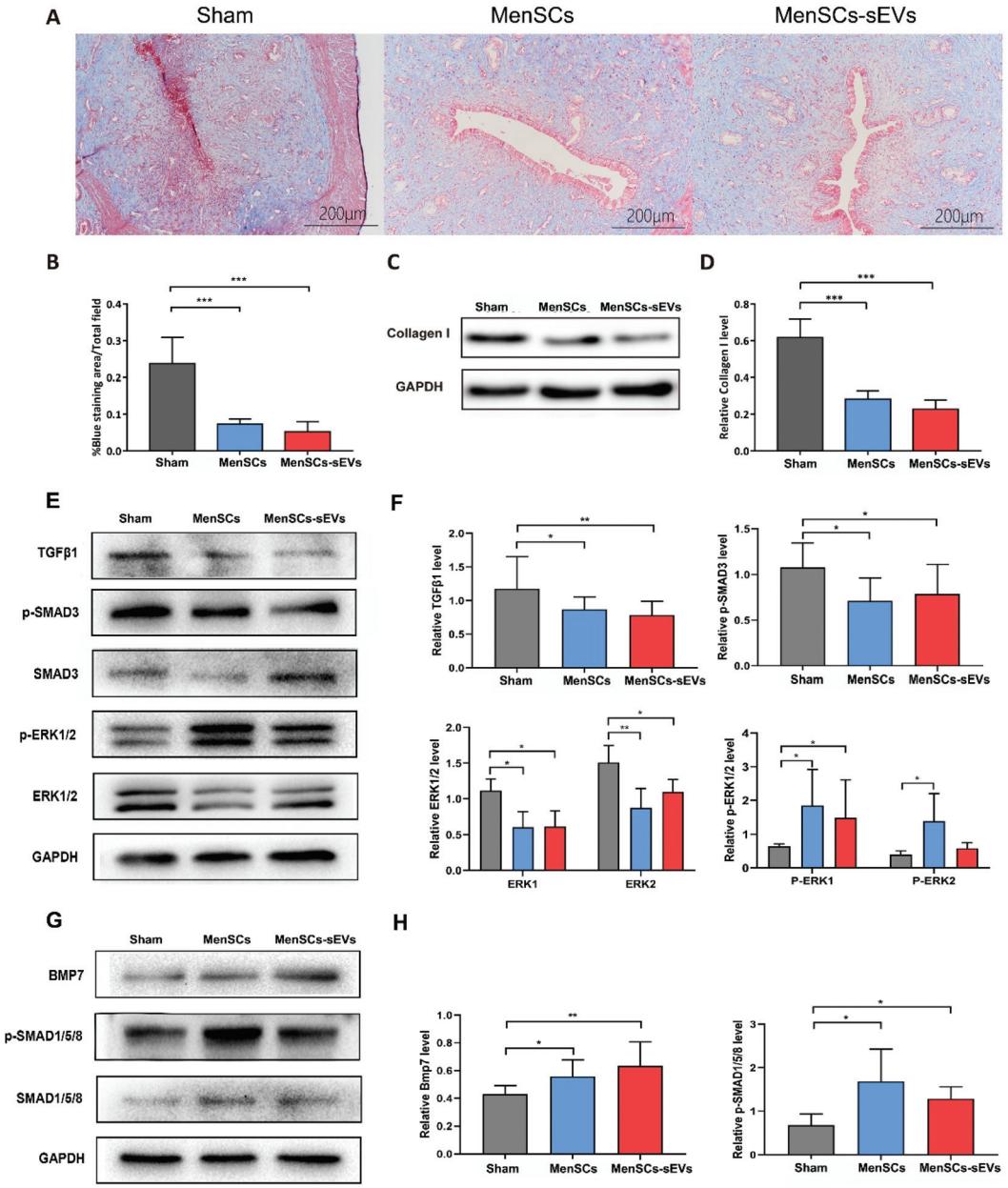

Fig. 6 MenSCs-sEVs inhibits fibrosis in IUA endometrium. (A) Representative Masson staining of rat endometrium after treatment for 4.5 days, scale bars = 200 μm; (B) comparison of the percentage of blue staining (fibrosis) area ($n \geq 6$); (C) the expression of collagen I proteins was detected by western blotting; (D) comparison of collagen I protein expression ($n \geq 6$); (E) western blot analysis of the protein expression of TGFβ1, *p*-SMAD3, SMAD3, *p*-ERK1/2 and ERK1/2 in the groups after treatment for 4.5 days; (F) statistical analysis of western blot ($n \geq 6$); (G) western blot analysis of the protein expression of BMP7, *p*-SMAD1/5/8 and SMAD1/5/8 in the groups after treatment for 4.5 days; and (H) statistical analysis of western blot ($n \geq 6$).

for clinical applications, with the advantages of high cloning efficacy, non-invasive collection, ethical rationale, and immunomodulatory potential.[8,15,20,21] Our phase 1 clinical study confirmed that autologous MenSCs effectively promoted endometrial repair and improved pregnancy outcomes in patients with severe IUA.[7] Recently, we reported that intrauterine transplantation of MenSCs is safe and free of organ toxicity and tumorigenicity.[16]

In clinical practice, we have observed that some patients with severe IUA have amenorrhea or scanty menstruation, making it difficult to obtain menstrual blood samples for the extraction of autologous MenSCs. Thus, stem cell product transplantation was suggested as a promising biological therapy. The paracrine effects of MSCs affect their main biological processes through the release of numerous EVs and soluble factors.[11,22] In murine models, the therapeutic effects

of MSC-derived exosomes (sEVs) have been demonstrated on liver fibrosis, hindlimb ischemia, retinal ischemia, nerve damage, and skin burns.[14,23–27] In this study, we demonstrated that the major functional proteins enriched by MenSCs-sEVs were clustered in signaling pathways (Wnt, ECM interaction, phosphatidylinositol 3-kinase–Akt, and integrin), and are involved in the regulation of cell proliferation and differentiation, epithelial development, angiogenesis, collagen fiber organization, and other biological processes. These results are consistent with the established mechanism of MSCs in the treatment of endometrial injuries.[8,28–30]

As of 2020, there are 14 clinical trials investigating the safety and efficiency of EVs from BMSCs, adipose-derived MSCs, and UC-MSCs in type I diabetes mellitus, bronchopulmonary dysplasia, periodontitis, chronic ulcer, and other conditions such as for wounds, acute type A aortic dissection, pulmonary infection, and Alzheimer's disease.[31] Most of these clinical trials are still in progress and no specific information can be obtained. As a preclinical study, this study confirmed the efficacy and safety of MenSCs-sEVs in the treatment of IUA. Intrauterine transplantation of MenSCs-sEVs restored endometrial function and fertility in rat models without causing changes in the blood cell composition or kidney and liver function abnormalities, suggesting that MenSCs-sEVs have potential clinical application in the treatment of endometrial injury.

To visually observe the roles of MenSCs and MenSCs-sEVs in endometrial regeneration, we first performed 3D fluorescence imaging of IUA uteruses using hydrophilic tissue clearing technology, which enabled the visualization of specific markers expressed in the 3D organ architecture.[32,33] Recent studies have demonstrated that MSC-derived EVs display injury tropism, concentrating in the damaged tissues in the murine models of acute kidney and spinal cord injury.[34,35] Similarly, our results indicated that MenSCs-sEVs effectively promoted the regeneration of glands and blood vessels around the transplant sites. In this study, the blood vessels regenerated after MenSCs or MenSCs-sEVs treatment, indicating their pro-angiogenic properties. We also observed co-localization of GFP and PECAM1 in the MenSCs group, which suggested that the injected MenSCs migrated to the nearby uterine endothelium, entered the bloodstream, and traveled along the uterine blood vessels. Higher fluorescence signals were detected in the brains and livers of IUA rats after GFP-MenSCs transplantation, indicating the vascular tropism of MenSCs. According to Kalionis *et al.*,[36] MSCs cross the endothelial barrier in a manner similar to that of leukocytes, and the transmigrated cells remain close to the endothelium. According to our recent study,[16] this spontaneous migration of MenSCs does not cause tumors or hypofunction in other organs.

Progressive fibrosis is a characteristic of IUA.[37] Recent studies demonstrated that MSC-derived EVs facilitate collagen degradation after renal ischemia-reperfusion injury and hepatic collagen deposition *in vivo*.[14,38] Our results indicate that MenSCs-sEVs significantly suppressed collagen deposition and reduced endometrial fibrosis at 4.5 days after treatment, consistent with the observations of a previous study that used human UC-MSC-derived EVs to treat IUA in rats.[39] The upregulation in the expression of the inflammation-related profibrotic molecule TGFβ1 has been shown to be positively correlated with the degree of IUA both in clinical endometrial samples and animal models.[40–42] Increased TGFβ1 expression is believed to be directly related to the occurrence and development of fibrosis, which may aggravate endometrial fibrosis through the SMAD3 signaling pathway.[43,44] Yao *et al.* reported that BMSC-derived EVs reversed endometrial fibrosis *via* inhibiting TGFβ1 activation and EMT *in vitro*.[45] In addition, studies on vitreoretinopathy and skin scars showed that upregulation of ERK1/2 has regulatory effects on TGFβ1-mediated fibrosis.[46,47] In the present study, we found that the phosphorylation of ERK1/2 was improved after MenSCs-sEVs treatment. In our previous study, RNA sequencing data revealed that *BMP7* expression was significantly upregulated after MenSCs transplantation.[8] BMP7 plays roles in fibrosis reversion and EMT inhibition in a variety of tissues.[48–50] In pulmonary and renal fibrosis, BMP7 facilitates scar repair by regulating SMAD1/5.[51,52] In this study, we confirmed that the protein expression of BMP7 and phosphorylation of SMAD1/5/8 were significantly increased after both MenSCs and MenSCs-sEVs transplantation. Guo *et al.* also indicated decreased expression of BMP7 and SMAD1/5 in the uterus of the IUA rat model, suggesting that BMP7 may be a potential target for IUA treatment.[53]

There are three limitations to our present study. First, our findings suggest that MenSCs-sEVs should be administered multiple times for therapeutic applications; thus, methods for improving the productivity or *in vivo* stability of MenSCs-sEVs warrant further research. Second, we locally injected the MenSCs-sEVs into the uterus; thus, the optimal route for exosome administration will require further exploration. Third, we did not conduct health and development testing of live-born cubs after MenSCs and MenSCs-sEVs treatments. Moreover, careful attention to the sterile production and storage of MenSCs-sEVs will be necessary to minimize risks. Owing to their biocompatibility and stability, MenSCs-sEVs offer a promising, cell-free, MSC-based therapy for IUA. Future studies on the clinical application of MenSCs-sEVs can focus on identifying their effective contents and improving their efficacy by administering them in combination with additional treatments.

In summary, our study demonstrated that transplantation of MenSCs-sEVs safely and effectively promoted the regeneration of endometrial glands and blood vessels, and improves fertility in IUA rats. Furthermore, treatment with MenSCs and MenSCs-sEVs increased BMP7 levels and activated the SMAD1/5/8 and ERK1/2 pathways *in vivo*, thereby alleviating endometrial fibrosis *via* inhibiting TGFβ1/SMAD3 signaling. Therefore, MenSCs-sEVs have therapeutic effects on endometrial injuries, suggesting an important role in the repair of IUA by MenSCs. Our findings provide insight into the mechanisms underlying the effects of MenSCs in endometrial regen-

eration and provide a theoretical basis for the use of MenSCs-sEVs in IUA treatment.

Ethics approval and consent to participate

All protocols were approved by the Ethics Committee of the Shengjing Hospital affiliated to China Medical University (2019PS349K) and were consistent with the principles of the Declaration of Helsinki.

Availability of data and materials

The data that support the findings of this study are available from the corresponding author upon reasonable request.

Funding

This study received funding from the National Natural Science Foundation of China (82071601), the Central Government Guidance for Local Science and Technology Development Projects for Liaoning Province (2020JH6/10500006), the National Natural Science Foundation of China (61873257), Science and Technology Program of Shenyang (20-205-4-011), the National Key Research and Development Program (2018YFC1002105), the Key Research and Development Program of Liaoning Province (2018020222), the Major Special Construction Plan for Discipline Construction Project of China Medical University (3110118033) and the Shengjing Freelance Researcher Plan of Shengjing Hospital of China Medical University.

Author contributions

SZ and QC conducted the experiments, collected and analyzed the data and prepared the manuscript; ZY and PL provided technical guidance; XT and YF conducted the three-dimensional imaging; XH and XZ participated in the western blot experiments; and JT designed the experiments, supervised the whole work and approved the final version of the manuscript. All authors read and approved the final manuscript.

Conflicts of interest

The authors declare that they have no competing interests.

Acknowledgements

We are particularly grateful to Aaron J.W. Hsueh and Yang Li for insightful comments and writing guidance. We are grateful to Chao Han for writing guidance.

References

1 D. Yu, Y. M. Wong, Y. Cheong, E. Xia and T. C. Li, *Fertil. Steril.*, 2008, **89**, 759–779.
2 E. M. Myers and B. S. Hurst, *Fertil. Steril.*, 2012, **97**, 160–164.
3 X. Santamaria, S. Cabanillas, I. Cervelló, C. Arbona, F. Raga, J. Ferro, J. Palmero, J. Remohí, A. Pellicer and C. Simón, *Hum. Reprod.*, 2016, **31**, 1087–1096.
4 L. Xu, L. Ding, L. Wang, Y. Cao, H. Zhu, J. Lu, X. Li, T. Song, Y. Hu and J. Dai, *Stem Cell Res. Ther.*, 2017, **8**, 84.
5 M. C. Rodrigues, T. Lippert, H. Nguyen, S. Kaelber, P. R. Sanberg and C. V. Borlongan, *Adv. Exp. Med. Biol.*, 2016, **951**, 111–121.
6 X. Chen, J. Sun, X. Li, L. Mao, L. Cui and W. Bai, *Stem Cell Res. Ther.*, 2019, **10**, 107.
7 J. Tan, P. Li, Q. Wang, Y. Li, X. Li, D. Zhao, X. Xu and L. Kong, *Hum. Reprod.*, 2016, **31**, 2723–2729.
8 S. Zhang, P. Li, Z. Yuan and J. Tan, *Stem Cell Res. Ther.*, 2019, **10**, 61.
9 A. Trounson and C. McDonald, *Cell Stem Cell*, 2015, **17**, 11–22.
10 C. Théry, K. W. Witwer, E. Aikawa, M. J. Alcaraz, J. D. Anderson, R. Andriantsitohaina, A. Antoniou, T. Arab, F. Archer, G. K. Atkin-Smith, D. C. Ayre, J. M. Bach, D. Bachurski, H. Baharvand, L. Balaj, S. Baldacchino, N. N. Bauer, A. A. Baxter, M. Bebawy, C. Beckham, A. Bedina Zavec, A. Benmoussa, A. C. Berardi, P. Bergese, E. Bielska, C. Blenkiron, S. Bobis-Wozowicz, E. Boilard, W. Boireau, A. Bongiovanni, F. E. Borràs, S. Bosch, C. M. Boulanger, X. Breakefield, A. M. Breglio, M. Brennan, D. R. Brigstock, A. Brisson, M. L. D. Broekman, J. F. Bromberg, P. Bryl-Górecka, S. Buch, A. H. Buck, D. Burger, S. Busatto, D. Buschmann, B. Bussolati, E. I. Buzás, J. B. Byrd, G. Camussi, D. R. F. Carter, S. Caruso, L. W. Chamley, Y. T. Chang, A. D. Chaudhuri, C. Chen, S. Chen, L. Cheng, A. R. Chin, A. Clayton, S. P. Clerici, A. Cocks, E. Cocucci, R. J. Coffey, A. Cordeiro-da-Silva, Y. Couch, F. A. W. Coumans, B. Coyle, R. Crescitelli, M. F. Criado, C. D'Souza-Schorey, S. Das, P. de Candia, E. F. de Santana, O. de Wever, H. A. del Portillo, T. Demaret, S. Deville, A. Devitt, B. Dhondt, D. di Vizio, L. C. Dieterich, V. Dolo, A. P. Dominguez Rubio, M. Dominici, M. R. Dourado, T. A. P. Driedonks, F. v. Duarte, H. M. Duncan, R. M. Eichenberger, K. Ekström, S. el Andaloussi, C. Elie-Caille, U. Erdbrügger, J. M. Falcón-Pérez, F. Fatima, J. E. Fish, M. Flores-Bellver, A. Försönits, A. Frelet-Barrand, F. Fricke, G. Fuhrmann, S. Gabrielsson, A. Gámez-Valero, C. Gardiner, K. Gärtner, R. Gaudin, Y. S. Gho, B. Giebel, C. Gilbert, M. Gimona, I. Giusti, D. C. I. Goberdhan, A. Görgens, S. M. Gorski, D. W. Greening, J. C. Gross, A. Gualerzi, G. N. Gupta, D. Gustafson, A. Handberg, R. A. Haraszti, P. Harrison, H. Hegyesi, A. Hendrix, A. F. Hill, F. H. Hochberg, K. F. Hoffmann, B. Holder, H. Holthofer, B. Hosseinkhani, G. Hu, Y. Huang, V. Huber, S. Hunt, A. G. E. Ibrahim,

T. Ikezu, J. M. Inal, M. Isin, A. Ivanova, H. K. Jackson, S. Jacobsen, S. M. Jay, M. Jayachandran, G. Jenster, L. Jiang, S. M. Johnson, J. C. Jones, A. Jong, T. Jovanovic-Talisman, S. Jung, R. Kalluri, S. ichi Kano, S. Kaur, Y. Kawamura, E. T. Keller, D. Khamari, E. Khomyakova, A. Khvorova, P. Kierulf, K. P. Kim, T. Kislinger, M. Klingeborn, D. J. Klinke, M. Kornek, M. M. Kosanović, Á. F. Kovács, E. M. Krämer-Albers, S. Krasemann, M. Krause, I. v. Kurochkin, G. D. Kusuma, S. Kuypers, S. Laitinen, S. M. Langevin, L. R. Languino, J. Lannigan, C. Lässer, L. C. Laurent, G. Lavieu, E. Lázaro-Ibáñez, S. le Lay, M. S. Lee, Y. X. F. Lee, D. S. Lemos, M. Lenassi, A. Leszczynska, I. T. S. Li, K. Liao, S. F. Libregts, E. Ligeti, R. Lim, S. K. Lim, A. Linē, K. Linnemannstöns, A. Llorente, C. A. Lombard, M. J. Lorenowicz, Á. M. Lörincz, J. Lötvall, J. Lovett, M. C. Lowry, X. Loyer, Q. Lu, B. Lukomska, T. R. Lunavat, S. L. N. Maas, H. Malhi, A. Marcilla, J. Mariani, J. Mariscal, E. S. Martens-Uzunova, L. Martin-Jaular, M. C. Martinez, V. R. Martins, M. Mathieu, S. Mathivanan, M. Maugeri, L. K. McGinnis, M. J. McVey, D. G. Meckes, K. L. Meehan, I. Mertens, V. R. Minciacchi, A. Möller, M. Møller Jørgensen, A. Morales-Kastresana, J. Morhayim, F. Mullier, M. Muraca, L. Musante, V. Mussack, D. C. Muth, K. H. Myburgh, T. Najrana, M. Nawaz, I. Nazarenko, P. Nejsum, C. Neri, T. Neri, R. Nieuwland, L. Nimrichter, J. P. Nolan, E. N. M. Nolte-'t Hoen, N. Noren Hooten, L. O'Driscoll, T. O'Grady, A. O'Loghlen, T. Ochiya, M. Olivier, A. Ortiz, L. A. Ortiz, X. Osteikoetxea, O. Ostegaard, M. Ostrowski, J. Park, D. M. Pegtel, H. Peinado, F. Perut, M. W. Pfaffl, D. G. Phinney, B. C. H. Pieters, R. C. Pink, D. S. Pisetsky, E. Pogge von Strandmann, I. Polakovicova, I. K. H. Poon, B. H. Powell, I. Prada, L. Pulliam, P. Quesenberry, A. Radeghieri, R. L. Raffai, S. Raimondo, J. Rak, M. I. Ramirez, G. Raposo, M. S. Rayyan, N. Regev-Rudzki, F. L. Ricklefs, P. D. Robbins, D. D. Roberts, S. C. Rodrigues, E. Rohde, S. Rome, K. M. A. Rouschop, A. Rughetti, A. E. Russell, P. Saá, S. Sahoo, E. Salas-Huenuleo, C. Sánchez, J. A. Saugstad, M. J. Saul, R. M. Schiffelers, R. Schneider, T. H. Schøyen, A. Scott, E. Shahaj, S. Sharma, O. Shatnyeva, F. Shekari, G. V. Shelke, A. K. Shetty, K. Shiba, P. R. M. Siljander, A. M. Silva, A. Skowronek, O. L. Snyder, R. P. Soares, B. W. Sódar, C. Soekmadji, J. Sotillo, P. D. Stahl, W. Stoorvogel, S. L. Stott, E. F. Strasser, S. Swift, H. Tahara, M. Tewari, K. Timms, S. Tiwari, R. Tixeira, M. Tkach, W. S. Toh, R. Tomasini, A. C. Torrecilhas, J. P. Tosar, V. Toxavidis, L. Urbanelli, P. Vader, B. W. M. van Balkom, S. G. van der Grein, J. van Deun, M. J. C. van Herwijnen, K. van Keuren-Jensen, G. van Niel, M. E. van Royen, A. J. van Wijnen, M. H. Vasconcelos, I. J. Vechetti, T. D. Veit, L. J. Vella, É. Velot, F. J. Verweij, B. Vestad, J. L. Viñas, T. Visnovitz, K. v. Vukman, J. Wahlgren, D. C. Watson, M. H. M. Wauben, A. Weaver, J. P. Webber, V. Weber, A. M. Wehman, D. J. Weiss, J. A. Welsh, S. Wendt, A. M. Wheelock, Z. Wiener, L. Witte, J. Wolfram, A. Xagorari, P. Xander, J. Xu, X. Yan, M. Yáñez-Mó, H. Yin, Y. Yuana, V. Zappulli, J. Zarubova, V. Žėkas, J. ye Zhang, Z. Zhao, L. Zheng, A. R. Zheutlin, A. M. Zickler, P. Zimmermann, A. M. Zivkovic, D. Zocco and E. K. Zuba-Surma, *J. Extracell. Vesicles*, 2018, **7**, 1535750.

11 S. Rani, A. E. Ryan, M. D. Griffin and T. Ritter, *Mol. Ther.*, 2015, **23**, 812–823.

12 D. G. Phinney and M. F. Pittenger, *Stem Cells*, 2017, **35**, 851–858.

13 C. Y. Chen, S. S. Rao, L. Ren, X. K. Hu, Y. J. Tan, Y. Hu, J. Luo, Y. W. Liu, H. Yin, J. Huang, J. Cao, Z. X. Wang, Z. Z. Liu, H. M. Liu, S. Y. Tang, R. Xu and H. Xie, *Theranostics*, 2018, **8**, 1607–1623.

14 T. Li, Y. Yan, B. Wang, H. Qian, X. Zhang, L. Shen, M. Wang, Y. Zhou, W. Zhu, W. Li and W. Xu, *Stem Cells Dev.*, 2013, **22**, 845–854.

15 F. Rossignoli, A. Caselli, G. Grisendi, S. Piccinno, J. S. Burns, A. Murgia, E. Veronesi, P. Loschi, C. Masini, P. Conte, P. Paolucci, E. M. Horwiz and M. Dominici, *BioMed Res. Int.*, 2013, **2013**, 901821.

16 Q. Y. Chang, S. W. Zhang, P. P. Li, Z. W. Yuan and J. C. Tan, *World J. Stem Cells*, 2020, **12**, 368–380.

17 T. Ma, P. Cui, X. Tong, W. Hu, L. R. Shao, F. Zhang, X. Li and Y. Feng, *Int. J. Mol. Sci.*, 2018, **19**, 11.

18 Y. Cao, H. Sun, H. Zhu, X. Zhu, X. Tang, G. Yan, J. Wang, D. Bai, J. Wang, L. Wang, Q. Zhou, H. Wang, C. Dai, L. Ding, B. Xu, Y. Zhou, J. Hao, J. Dai and Y. Hu, *Stem Cell Res. Ther.*, 2018, **9**, 192.

19 L. de Miguel-Gómez, H. Ferrero, S. López-Martínez, H. Campo, N. López-Pérez, A. Faus, D. Hervás, X. Santamaría, A. Pellicer and I. Cervelló, *BJOG*, 2020, **127**, 551–560.

20 F. Alcayaga-Miranda, J. Cuenca, P. Luz-Crawford, C. Aguila-Díaz, A. Fernandez, F. E. Figueroa and M. Khoury, *Stem Cell Res. Ther.*, 2015, **6**, 32.

21 S. Darzi, J. A. Werkmeister, J. A. Deane and C. E. Gargett, *Stem Cells Transl. Med.*, 2016, **5**, 1127–1132.

22 S. Keshtkar, N. Azarpira and M. H. Ghahremani, *Stem Cell Res. Ther.*, 2018, **9**, 63.

23 P. Gangadaran, R. L. Rajendran, H. W. Lee, S. Kalimuthu, C. M. Hong, S. Y. Jeong, S. W. Lee, J. Lee and B. C. Ahn, *J. Controlled Release*, 2017, **264**, 112–126.

24 B. Mathew, S. Ravindran, X. Liu, L. Torres, M. Chennakesavalu, C. C. Huang, L. Feng, R. Zelka, J. Lopez, M. Sharma and S. Roth, *Biomaterials*, 2019, **197**, 146–160.

25 B. Zhang, M. Wang, A. Gong, X. Zhang, X. Wu, Y. Zhu, H. Shi, L. Wu, W. Zhu, H. Qian and W. Xu, *Stem Cells*, 2015, **33**, 2158–2168.

26 M. A. Lopez-Verrilli, A. Caviedes, A. Cabrera, S. Sandoval, U. Wyneken and M. Khoury, *Neuroscience*, 2016, **320**, 129–139.

27 L. Chen, B. Xiang, X. Wang and C. Xiang, *Stem Cell Res. Ther.*, 2017, **8**, 9.

28 Y. Zhang, X. Lin, Y. Dai, X. Hu, H. Zhu, Y. Jiang and S. Zhang, *Reproduction*, 2016, **152**, 389–402.

29 J. Yu, L. Jiang, Y. Gao, Q. Sun, B. Liu, Y. Hu and X. Han, *Am. J. Transl. Res.*, 2018, **10**, 4280–4289.

30 S. Zhao, W. Qi, J. Zheng, Y. Tian, X. Qi, D. Kong, J. Zhang and X. Huang, *Reprod. Sci.*, 2020, **27**, 1266–1275.
31 M. Massa, S. Croce, R. Campanelli, C. Abbà, E. Lenta, C. Valsecchi and M. A. Avanzini, *Diagnostics*, 2020, **10**, 12.
32 H. Kolesová, M. Čapek, B. Radochová, J. Janáček and D. Sedmera, *Histochem. Cell Biol.*, 2016, **146**, 141–152.
33 J. Seo, M. Choe and S. Y. Kim, *Mol. Cells*, 2016, **39**, 439–446.
34 K. L. Lankford, E. J. Arroyo, K. Nazimek, K. Bryniarski, P. W. Askenase and J. D. Kocsis, *PLoS One*, 2018, **13**, e0190358.
35 C. Grange, M. Tapparo, S. Bruno, D. Chatterjee, P. J. Quesenberry, C. Tetta and G. Camussi, *Int. J. Mol. Med.*, 2014, **33**, 1055–1063.
36 B. Al-Sowayan, R. J. Keogh, M. Abumaree, H. M. Georgiou and B. Kalionis, *Stem Cell Invest.*, 2019, **6**, 2.
37 R. Deans and J. Abbott, *J. Minim. Invasive Gynecol.*, 2010, **17**, 555–569.
38 X. Zou, D. Gu, X. Xing, Z. Cheng, D. Gong, G. Zhang and Y. Zhu, *Am. J. Transl. Res.*, 2016, **8**, 4289–4299.
39 N. Ebrahim, O. Mostafa, R. E. El Dosoky, I. A. Ahmed, A. S. Saad, A. Mostafa, D. Sabry, K. A. Ibrahim and A. S. Farid, *Stem Cell Res. Ther.*, 2018, **9**, 175.
40 A. F. Muro, F. A. Moretti, B. B. Moore, M. Yan, R. G. Atrasz, C. A. Wilke, K. R. Flaherty, F. J. Martinez, J. L. Tsui, D. Sheppard, F. E. Baralle, G. B. Toews and E. S. White, *Am. J. Respir. Crit. Care Med.*, 2008, **177**, 638–645.
41 Q. Zhou, X. Wu, J. Hu and R. Yuan, *Int. J. Mol. Med.*, 2018, **42**, 81–90.
42 X. Bai, J. Liu, W. Yuan, Y. Liu, W. Li, S. Cao, L. Yu and L. Wang, *Cell Transplant.*, 2020, **29**, 963689720908495.
43 J. Cao, D. Liu, S. Zhao, L. Yuan, Y. Huang, J. Ma, Z. Yang, B. Shi, L. Wang and J. Wei, *Braz. J. Med. Biol. Res.*, 2020, **53**, e9794.
44 U. Salma, M. Xue, M. S. Ali Sheikh, X. Guan, B. Xu, A. Zhang, L. Huang and D. Xu, *Mediators Inflammation*, 2016, **2016**, 4158287.
45 Y. Yao, R. Chen, G. Wang, Y. Zhang and F. Liu, *Stem Cell Res. Ther.*, 2019, **10**, 225.
46 O. K. Hong, S. S. Lee, S. J. Yoo, M. K. Lee, M. K. Kim, K. H. Baek, K. H. Song and H. S. Kwon, *Endocrinol. Metab.*, 2020, **35**, 384–395.
47 C. C. Darmawan, S. E. Montenegro, G. Jo, N. Kusumaningrum, S. H. Lee, J. H. Chung and J. H. Mun, *Int. J. Mol. Sci.*, 2020, **21**, 8.
48 A. C. Midgley, Y. Wei, D. Zhu, F. Gao, H. Yan, A. Khalique, W. Luo, H. Jiang, X. Liu, J. Guo, C. Zhang, G. Feng, K. Wang, X. Bai, W. Ning, C. Yang, Q. Zhao and D. Kong, *J. Am. Soc. Nephrol.*, 2020, **31**, 2292–2311.
49 C. Cai, S. Kilari, A. K. Singh, C. Zhao, M. L. Simeon, A. Misra, Y. Li and S. Misra, *J. Am. Heart Assoc.*, 2020, **9**, e017420.
50 Y. Song, S. Lv, F. Wang, X. Liu, J. Cheng, S. Liu, X. Wang, W. Chen, G. Guan, G. Liu and C. Peng, *Mol. Med. Rep.*, 2020, **21**, 833–841.
51 T. Zhang, J. Dai, W. Ye, L. Cai, J. Wei, M. Chen, X. Huang and X. Wang, *Biochem. Biophys. Res. Commun.*, 2020, **527**, 662–667.
52 X. Ji, J. Cao, L. Zhang, Z. Zhang, W. Shuai and W. Yin, *Biol. Pharm. Bull.*, 2020, **43**, 533–539.
53 L. P. Guo, L. M. Chen, F. Chen, N. H. Jiang and L. Sui, *Am. J. Transl. Res.*, 2019, **11**, 4726–4737.